Advances in Engineering Software 40 (2009) 1047–1055

Contents lists available at ScienceDirect

Advances in Engineering Software

journal homepage: www.elsevier.com/locate/advengsoft

Numerical analyses of embankments on PVD improved soft clays

Abdulazim Yildiz *

Department of Civil Engineering, The Faculty of Engineering and Architecture, Çukurova University, 01330 Balcali, Adana, Turkey

ARTICLE INFO

Article history:
Received 23 January 2009
Received in revised form 3 March 2009
Accepted 11 March 2009
Available online 10 April 2009

Keywords:
Finite element method
Prefabricated vertical drains
Soft clay
Anisotropy
Destructuration

ABSTRACT

In this paper, three-dimensional behaviour of an embankment on soft soils incorporating prefabricated vertical drains is analysed with finite element method using a recently proposed constitutive model, namely S-CLAY1S. The constitutive model accounts for plastic anisotropy, interparticle bonding and degradation of bonds. The numerical simulations show that neglecting effects of anisotropy and destructuration may lead to inaccurate predictions of soft clay response. The same problem is also analysed under two-dimensional plane strain conditions. Axisymmetric vertical drains are converted into equivalent plane strain conditions using three different numerical matching techniques purposed in the literature. In order to validate these matching techniques, the 2D equivalent plane strain results are compared with the results of 3D analysis. It is shown that these numerical matching techniques accurately predict the consolidation behaviour of an embankment on PVD improved soft clays and provide a useful tool for engineering practice.

1. Introduction

Numerical simulations by means of the Finite Element Method (FEM) have become a valuable tool in geotechnical engineering to predict and to understand the behaviour of complex structures and extensive research has been recently carried out in this area [1–5]. The construction and consolidation behaviour of an embankment with vertical drains has been usually analysed by the finite element method [6–8]. Stability and time required for consolidation are two major considerations in the design and construction of embankments over soft cohesive foundations [9]. Installing a drainage material vertically into the ground can shorten drainage path of soft clay deposits significantly and improve stiffness and strength of the ground substantially in a short period [10]. The true modelling of an embankment involving a large number of discrete vertical drains and their own independent influence zone requires three-dimensional (3D) analyses. However, 3D analyses are sophisticated and require large computational effort when applied to a real embankment project with a large number of vertical drains [11]. The actual 3D problem can be converted into an equivalent plane strain model which has equivalent properties and dimensions. Several authors [12–16] developed numerical matching techniques for simulating the vertical drain effect under two-dimensional (2D) plane strain conditions. These matching techniques assume that the consolidation behaviour takes place in an independent single drainage system (unit cell concept) which has linear compressibility characteristics without any lateral movements. Such restrictive conditions do not represent real soft soil behaviour and actual field conditions. The stress–strain behaviour of natural soft soils is highly nonlinear and very complex. Fundamental features of soil, such as anisotropy, creep and destructuration are also quite different. Therefore, it is necessary to consider real soil behaviour and multiple vertical drains under an embankment in the numerical analyses. In this paper, some matching techniques are applied to full scale analysis of an embankment on soft clay improved with vertical drains. In the finite element analyses, soft clays are modelled by a recently proposed elasto-plastic constitutive model, S-CLAY1S [17]. The model accounts for plastic anisotropy combined with destructuration. For comparison, the problem is also analysed with isotropic Modified Cam Clay (MCC) model [18]. In order to validate these equivalent plane strain models 3D full scale consolidation analyses are performed using PLAXIS finite element program. 3D analyses results are also compared with those of 2D analyses.

2. Constitutive model

Natural soft clay structure consists of fabric and interparticle bonding. The fabric (i.e. the arrangement of particles and particle contacts) is often anisotropic due to the shape of clay platelets, the deposition process and subsequent consolidation. The bonding between particles originates from the mineral and pore water compositions at the time of deposition, changes in environmental conditions and complex geo-chemical processes. Plastic straining causes slippage of particles and, hence, changes in anisotropy and bonding. The changes in anisotropy depend on the loading path. The interparticle bonding, which gives the soil additional

* Tel./fax: +90 322 338 67 02; mobile: +90 506 308 61 40.
E-mail address: azim@cukurova.edu.tr

0965-9978/$ - see front matter © 2009 Elsevier Ltd. All rights reserved.
doi:10.1016/j.advengsoft.2009.03.011

strength, degrades due to plastic straining and this process is called destructuration. The recently proposed elasto-plastic constitutive model called S-CLAY1S [17] describes initial anisotropy with an inclined yield surface and the changes in anisotropy via plastic strain-induced rotation of the yield surface. In addition, the model accounts for destructuration.

The S-CLAY1S model is an extension of the critical state models and the yield surface in 3D stress space is defined as

$$f = \frac{3}{2}\left[\{\underline{\sigma}_d - p'\underline{\alpha}_d\}^T\{\underline{\sigma}_d - p'\underline{\alpha}_d\}\right] - \left[M^2 - \frac{3}{2}\{\underline{\alpha}_d\}^T\{\underline{\alpha}_d\}\right](p'_m - p')p' = 0 \quad (1)$$

where σ_d is the deviatoric stress tensor, p' is the mean effective stress, α_d is a deviatoric fabric tensor (a dimensionless second order tensor that is defined analogously to the deviatoric stress tensor), M is the value of the stress ratio at the critical state and p'_m defines the size of the yield surface of the natural clay. Eq. (1) shows that the generalized version of the yield surface cannot be expressed solely in terms of stress invariants. Fig. 1a illustrates the shape of the S-CLAY1S yield surface in three-dimensional stress space for the case where the principal axes of both the stress tensor and the fabric tensor coincide with x, y and z directions.

Within the yield surface there is a notional "intrinsic yield surface" for the equivalent unbonded soil with the same fabric which is assumed to be of the same shape and orientation as the real yield surface, but smaller in size. The size of the intrinsic yield surface is specified by a parameter p'_{mi}, and this is related to the size p'_m of the yield surface for the natural soil by parameter χ, defining the current degree of bonding:

$$p'_m = (1 + \chi)p'_{mi} \quad (2)$$

For the simplified conditions of a triaxial test on a one-dimensional consolidated sample it can be assumed that the horizontal plane in the triaxial sample coincides with the plane of isotropy of the sample. In this special case, the fabric tensor can be replaced by a scalar parameter α defined as

$$\alpha^2 = \frac{3}{2}\{\underline{\alpha}_d\}^T\{\underline{\alpha}_d\} \quad (3)$$

which is a measure of the degree of plastic anisotropy of the soil. The yield curves of the S-CLAY1S model can then be visualized by Fig. 1b. For the sake of simplicity, the S-CLAY1S model assumes isotropic elastic behaviour of the same form as in the MCC model [18] and an associated flow rule.

S-CLAY1S incorporates three hardening laws. The first of these relates the change in the size of the intrinsic yield surface to the plastic volumetric strain increment $d\varepsilon_v^p$:

$$dp'_{mi} = \frac{vp'_{mi}}{\lambda_i - \kappa}d\varepsilon_v^p \quad (4)$$

where λ_i is the gradient of the intrinsic normal compression line (for a reconstituted soil) in the $\ln p'$–v plane (where v is the specific volume). Eq. (4) is of the same form as the equivalent hardening law in MCC and S-CLAY1, but with p'_m replaced by p'_{mi} and λ replaced by λ_i.

The second hardening law (the rotational hardening law) describes the change of orientation of the yield surface with plastic straining:

$$D\underline{\alpha}_d = \omega\left(\left[\frac{3\underline{\eta}}{4} - \underline{\alpha}_d\right]\langle d\varepsilon_v^p\rangle + \omega_d\left[\frac{\underline{\eta}}{3} - \underline{\alpha}_d\right]d\varepsilon_d^p\right) \quad (5)$$

where $\underline{\eta} = \underline{\sigma}_d/p'$, $d\varepsilon_d^p$ is the increment of plastic deviatoric strain ω and ω_d are additional soil constants. The soil constant ω_d controls the relative effectiveness of plastic shear strains in setting the overall instantaneous target values for the components of $\underline{\eta}_d$, whereas the soil constant ω controls the absolute rate of rotation of the yield surface towards the current target values of the components of $\underline{\eta}_d$ (see Wheeler et al. [19] for details).

The third hardening law in S-CLAY1S (the destructuration law) describes the degradation of bonding with plastic straining. It is similar in form to the rotational hardening law (Eq. (5)) except that both plastic volumetric strains and plastic shear strains (whether positive or negative) tend to decrease the value of the bonding parameter χ towards a target value of zero:

$$d\chi = \xi([0 - \chi]|d\varepsilon_v^p| + \xi_d[0 - \chi]d\varepsilon_d^p) = -\xi\chi(|d\varepsilon_v^p| + \xi_d d\varepsilon_d^p) \quad (6)$$

where ξ and ξ_d are additional soil constants. Parameter ξ controls the absolute rate of destructuration and parameter ξ_d controls the relative effectiveness of plastic deviatoric strains in destroying the bonding (see Koskinen et al. [20] for details). The S-CLAY1S model has been successfully validated against experimental data on several natural and reconstituted clays [20–23].

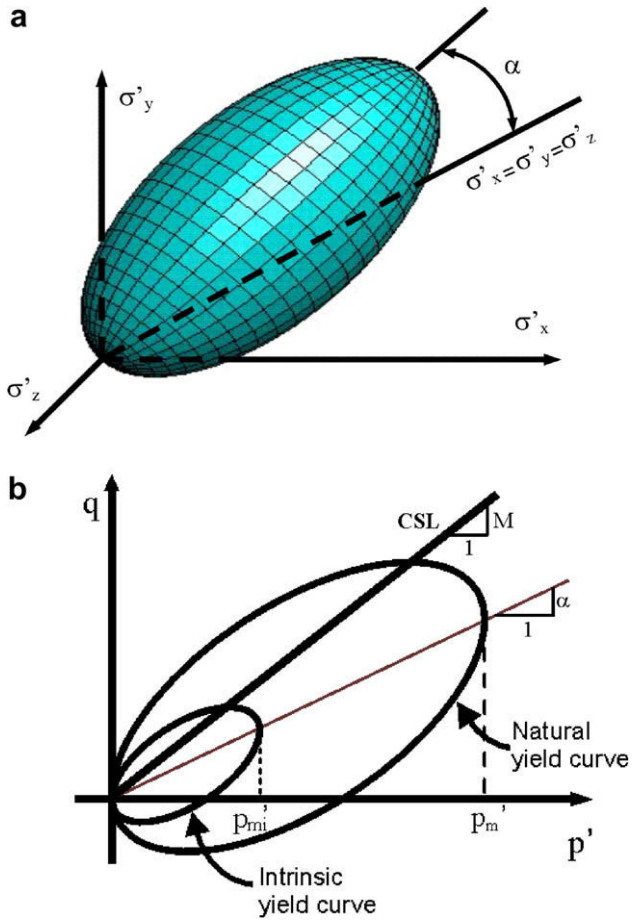

Fig. 1. S-CLAY1S yield surface in (a) three-dimensional stress space; (b) triaxial stress space.

3. Description of the benchmark problem

The geometry of the embankment is shown in Fig. 2. The soft soil is assumed to have the properties of POKO clay from Finland [20,21,24]. The ground water table is located 2 m below the ground surface. The boundaries of the geometry used in the finite element analyses have an extent of 40 m in the horizontal direction from the symmetry axis and 36 m in the vertical direction. The lateral boundaries are restrained horizontally and the bottom boundary is restrained in both directions. Drainage boundaries are assumed

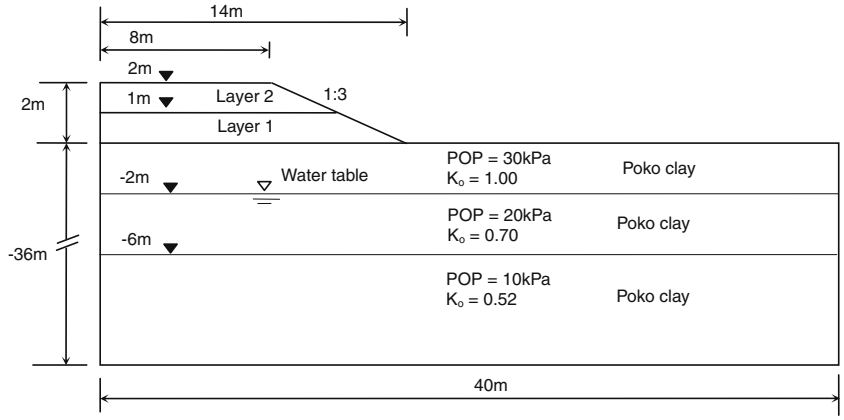

Fig. 2. Geometry of benchmark embankment and assumed soil profile.

to be at the level of the water table and at the bottom of the mesh, whereas the lateral boundaries are closed. Due to symmetry, only half of the embankment is represented in the finite element mesh. First, the embankment loading is applied under undrained conditions, assuming the embankment and the soil above the water table to be drained materials. Next, a consolidation phase is simulated via fully coupled static consolidation analyses. Mesh sensitivity studies were done to confirm that the mesh was dense enough to give accurate results for all of the constitutive models concerned.

4. Model parameters

The embankment which is assumed to be made of granular fill was modelled with a simple Mohr Coulomb model assuming the following material parameters: $E' = 40{,}000$ kN/m^2, $\nu' = 0.3$, $\psi' = 38°$, $\psi' = 0°$, $c' = 1$ kN/m^2 and $\gamma = 20$ kN/m^3, where E' is the secant stiffness modulus, ν' is the Poisson's ratio, ψ' is the dilatancy angle and γ is the unit weight of the embankment material.

The soft soil profile corresponds to the so-called POKO clay [20,21]. The abbreviation POKO stands for Porvoo-Koskenkylä, a 25 km long section of motorway construction near the medieval town of Porvoo, Finland. For the benchmark simulations the deposit was idealized by using a single set of soil parameters throughout with an overconsolidation profile that approximates the conditions at the site. The deposit was modelled as a lightly overconsolidated soft clay with vertical pre-overburden pressure (POP) values and in situ K_0 values varying with the depth as shown in Table 1. The vertical pre-overburden pressure is defined as $\mathrm{POP} = \sigma'_p - \sigma'_{v0}$ (where σ'_{v0} and σ'_p are the in situ value and maximum past value of the vertical effective stress, respectively). The in situ stresses were estimated assuming a bulk unit weight of 15 kN/m^3. The permeability of the soil was assumed to be 10^{-9} m/s in both vertical and horizontal directions for all analyses. The values of the input parameters and additional state variables for three models are shown in Table 2. The values have been determined systematically from odometer and triaxial tests on natural and reconstituted POKO clay [20,21]. The values for the initial inclination of the yield surface α_0 and parameter ω were determined by following the procedure described in Wheeler et al. [19], using K_0^{NC} values corresponding to Jaky's simplified formula. The initial value for x_0 was estimated based on sensitivity as suggested in Koskinen et al. [20,21]. For soil constants ω_d, ξ and ξ_d typical values for POKO clay have been assumed. In PLAXIS it is possible to allow for the decrease in the permeability as the void ratio decreases, using the formula suggested by Taylor [25]:

$$\log\left(\frac{k}{k_0}\right) = \frac{\Delta e}{c_k} \tag{7}$$

where Δe is a change in void ratio, k is the soil permeability in the calculation step, k_0 is the initial value of the permeability and c_k is the permeability change index. It was assumed that $c_k = 0.5e_0$ in the calculations [26].

Table 1
The initial values for the state parameters.

Layer	Depth (m)	e_0	POP (kN/m^2)	α_0	χ_0
1	0.0–2.0	2.1	30	0.46	12
2	2.0–6.0	2.1	20	0.46	12
3	6.0–36.0	2.1	10	0.46	12

Table 2
Soil constants for MCC and S-CLAY1S models.

Model	λ (or λ_i)	κ	ν'	M	ω	ω_d	ξ	ξ_d
MCC	0.71	0.03	0.2	1.2	–	–	–	–
S-CLAY1S	0.26	0.03	0.2	1.2	20	0.76	9	0.2

Prefabricated vertical drains (PVD) are a slender, synthetic drainage element comprised of a drainage core wrapped in a geotextile filter. PVDs usually have rectangular cross-section (band-shaped). The conventional theory of radial consolidation assumes that drains are circular. Therefore, the rectangular section needs to be converted to an equivalent cylindrical drain with a circular influence zone. It is assumed that a PVD has cylindrical shape and its equivalent diameter d_w is 0.2 m in the finite element analyses (Fig. 3). PVDs are also assumed to be of 15 m length and installed in a square grid with 2 m spacing underneath the embankment. In the 3D full scale analyses the PVDs are modelled with a simple linear elastic model assuming $E = 100$ kN/m^2 and $\nu' = 0.2$. The permeability values of a PVD element are assumed to be isotropic and equal to 150 m/day to ignore well resistance in the analyses. It is not intended that the PVD reproduces any commercial product and these parameters are selected for the sake of simplicity in the analyses.

In the field, the installation of PVDs by means of a mandrel causes significant remoulding of the subsoil, especially in the immediate vicinity of the mandrel. The resulting smear zone will have reduced lateral permeability, which adversely affects consolidation process [15] and hence, the smear effect must be taken into consideration in the finite element analyses (Fig. 4). Two parameters are necessary to characterize the smear effect; namely, the diameter of the smear zone (d_s) and the permeability ratio (k_h/k_s), i.e., the value in the undisturbed zone (k_h) over the smear zone

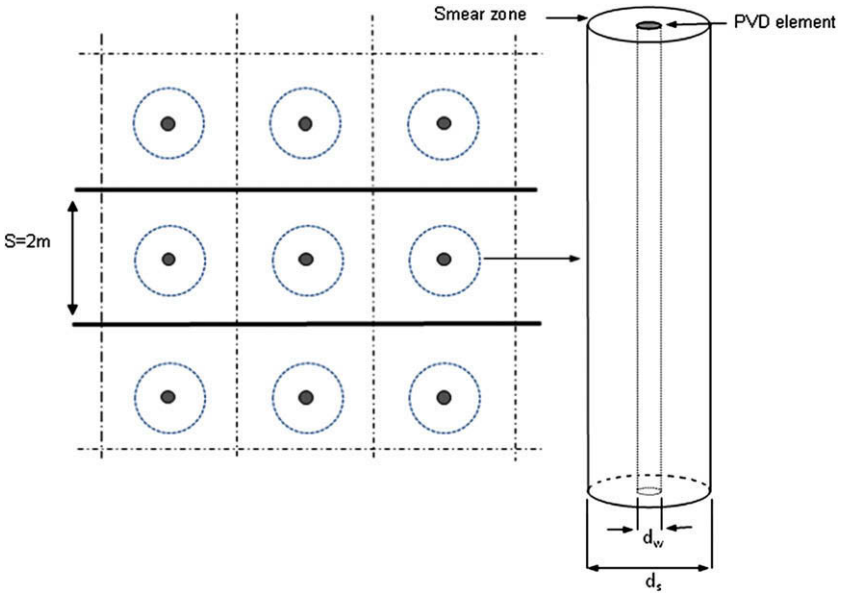

Fig. 3. Drain installation pattern.

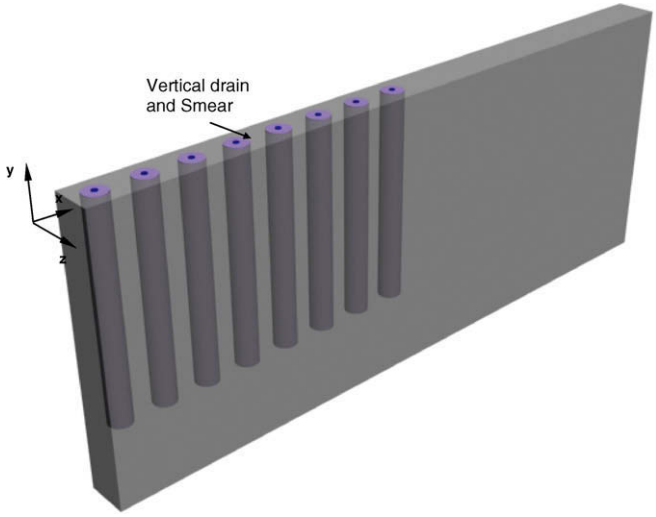

Fig. 4. 3D model of vertical drains.

(k_s). Both the diameter of the smear zone and its permeability are difficult to quantify. They cannot be easily determined from laboratory tests, either. To the best of the author's knowledge, there is no comprehensive or standard method to measure them. The effects have been found to vary with the installation procedure, size and shape of the mandrel and soil micro-fabric [27]. Several researchers have investigated these factors [28–31]. However, it is seen that there is no general agreement in the literature and Poko clay can be characterised as sensitive anisotropic soft clay. Hence, considerable disturbance may be expected in the subsoil during the installation of vertical drains. In the following analysis, the diameter of the smear zone (d_s) and the horizontal permeability in the smear zone were assumed to be $d_s = 4d_w$ [31] and $k_h/k_s = 10$ [30], respectively. Well resistance refers to the finite permeability of the vertical drain with respect to the soil. In general, laboratory and field data indicate that the discharge capacities of most commercial PVDs have little influence on the consolidation rate of clay and well resistance can be ignored for PVD < 15 m long in most soft clays [31].

5. Finite element analyses

5.1. Three-dimensional analyses

The finite element mesh used for 3D numerical simulations is illustrated in Fig. 5. The 15-node wedge elements were used to model foundation soils in the analysis. The 15-node wedge element is composed of 6-node triangles in horizontal direction and 8-node quadrilaterals in vertical direction. The finite element mesh consists of 9732 elements. Each vertical drain and its own smear zone under the embankment were discretely modelled by creating volume pile elements with a circular cross-section. Therefore, a circular tube was used to create a cylindrical volume pile element in

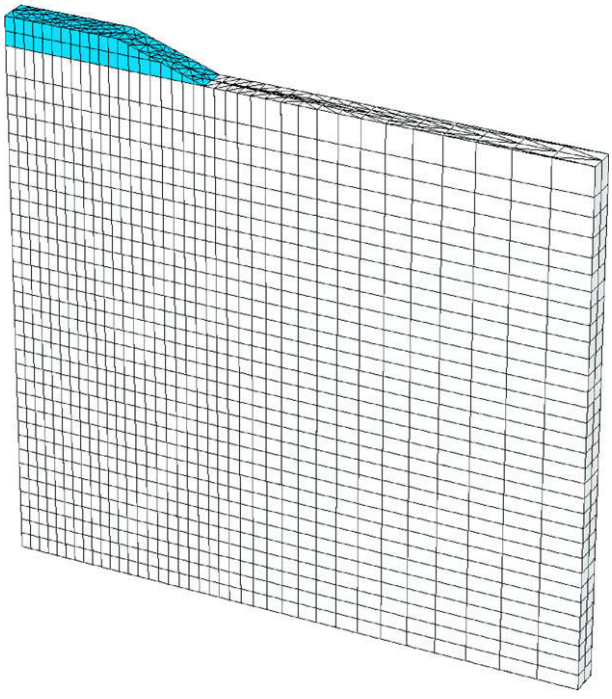

Fig. 5. Finite element mesh for 3D analyses.

the finite element program. A vertical drain and its smear zone were specified by means of the inner diameter (d_w) and thickness of circular tube ($d_s - d_w$), respectively (Fig. 3).

5.2. Two-dimensional analyses

Three different matching techniques proposed by Hird et al. [14], Indraratna and Redana [15] and Chai et al. [16] were adopted for equivalent plane strain analyses. Fig. 6 shows an axisymmetric unit cell with the total radius (R) and its equivalent plane strain unit cell with half-width (B). The effective diameter of a drain influence was calculated as 2.26 m by using $D_e = 1.13S$ for a square configuration where S is the drain spacing [32]. The equivalent drain radius (r_w) and unit cell radius (R) were calculated as 0.10 and 1.13 m, respectively.

Based on Hansbo's [33] solution, Hird et al. [14] showed that the average degree of consolidation U, at any depth and time in the two unit cells (axisymmetric and plane strain) were theoretically identical and the matching can be achieved by any one of three methods: (i) geometric mapping – the drain spacing is matched while maintaining the same permeability coefficient; (ii) permeability mapping – coefficient of permeability is matched while keeping the same drain spacing; and (iii) combination of (i) and (ii), with the plane strain permeability calculated for a convenient drain spacing. According to Yildiz et al. [34], three matching procedures proposed by Hird et al. [14] produced effectively identical settlement response. Thus, combined mapping procedure is adopted as it seems to be the most convenient one allowing the control of the mesh geometry. In this approach, a value of B (half-width of unit cell) is preselected and the equivalent plane strain permeability k_{pl} is calculated by the following equation:

$$\frac{k_{pl}}{k_{ax}} = \frac{2B^2}{3R^2\left[\ln\left(\frac{R}{r_s}\right) + \left(\frac{k_{ax}}{k_s}\right)\ln\left(\frac{r_s}{r_w}\right) - \left(\frac{3}{4}\right)\right]} \tag{8}$$

where k_{ax} and k_s are the horizontal permeabilities of the undisturbed and disturbed soil, respectively. In the equivalent plane strain analyses, $B = 1$ m was preselected and the value of k_{pl} is calculated as $0.019k_{ax}$ by using Eq. (8). The finite element mesh used for the equivalent plane strain analyses is illustrated in Fig. 7a. A special drain element is used to model a vertical drain in the analyses where excess pore pressures are set to zero. This matching method has an important advantage that no smear zone needs to be represented in the plane strain model. The finite element mesh for the equivalent plane strain analyses consists of 530 15-noded triangular elements.

Indraratna and Redana [15] converted the vertical drain system into an equivalent parallel drain wall by adjusting the coefficient of soil permeability. They assumed that the half-widths of unit cell B, of drains b_w, and of smear zone b_s are the same as their axisymmetric radii R, r_w and r_s, respectively. Ignoring the well resistance, the equivalent permeability of the model is then determined by

$$\frac{k'_{hp}}{k_{hp}} = \frac{\beta}{\left[\ln\left(\frac{n}{s}\right) + \left(\frac{k_h}{k'_h}\right)\ln(s) - 0.75 - \alpha\right]} \tag{9}$$

where k_h is the horizontal permeability of the undisturbed soil and k'_h is the horizontal permeability of disturbed soil, where the subscript p represents the plane strain condition. The associated geometric parameters α and β are given by

$$\alpha = \frac{2}{3}\frac{(n-s)^3}{(n-1)n^2} \tag{10}$$

$$\beta = \frac{2}{3}\frac{(s-1)}{(n-1)n^2}\left[3n(n-s-1) + (s^2+s+1)\right] \tag{11}$$

where $n = R/r_w$ and $s = r_s/r_w$. The finite element mesh used for the equivalent plane strain analyses is illustrated in Fig. 7b. Both vertical drains and their own smear zones need to be discretely represented. A special drain element is used to model a vertical drain where excess pore pressures are set to zero. When the half-width (B) of the unit cell is taken as 1 m the values of k_{hp} and k'_{hp} are calculated as $0.33k_h$ and $0.013k_h$ in the undisturbed and disturbed zones, respectively by using Eq. (9). The finite element mesh consists of 858 15-noded triangular elements.

Chai et al. [16] mentioned that PVDs increase the mass hydraulic conductivity of subsoil in the vertical direction. Therefore, it is logical to try to establish a value of vertical hydraulic conductivity, which approximately represents both the effect of vertical

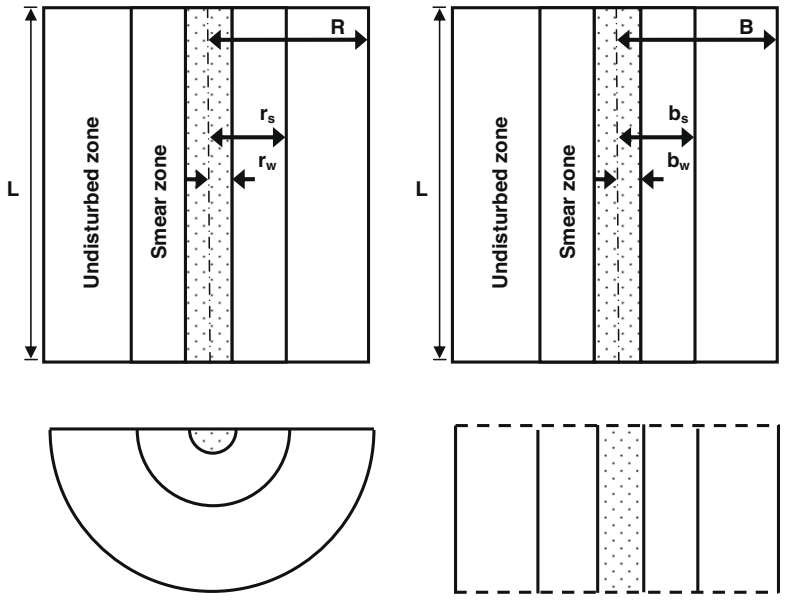

(a) Axisymmetric unit cell (b) Plane strain unit cell

Fig. 6. Axisymmetric unit cell and its equivalent plane strain unit cell.

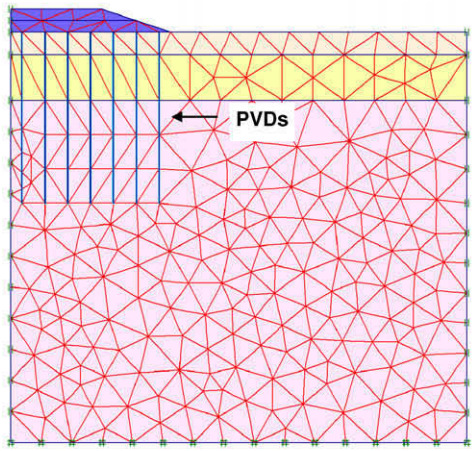

(a) FE mesh with Hird *et al.* [14]

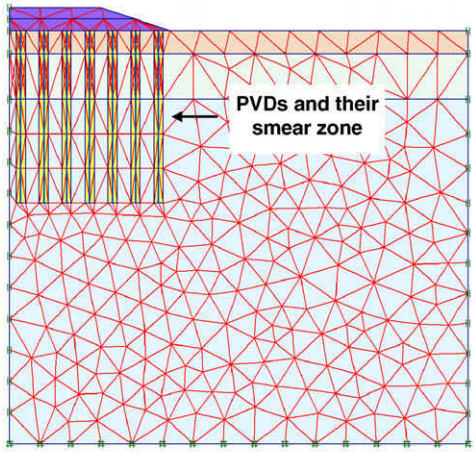

(b) FE mesh with Indraratna and Redana [15]

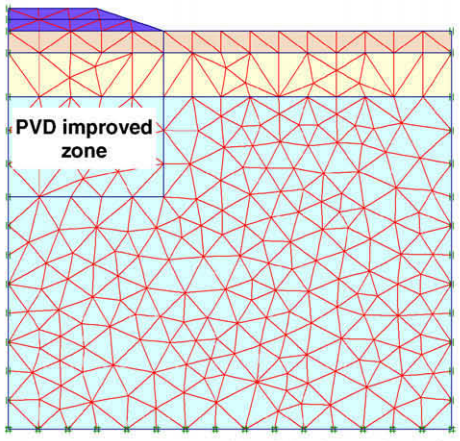

(c) FE mesh with Chai *et al.* [16]

Fig. 7. Finite element mesh for plane strain analyses.

drainage of natural subsoil and the effect of radial drainage due to existence of PVD. Under this condition, the PVD-improved subsoil can be analysed in the same way as the unimproved case. This equivalent value of vertical hydraulic conductivity k_{ve} is derived based on the equal average degree of consolidation under the 1D condition purposed by Carrillo [35]. The equivalent vertical hydraulic conductivity k_{ve} can be expressed as

$$k_{ve} = \left(1 + \frac{2.5l^2}{\mu D_e^2}\frac{k_h}{k_v}\right)k_v \tag{12}$$

where k_v = hydraulic conductivity in the vertical direction, l = drainage length, D_e = diameter of unit cell. The value of μ can be expressed as

$$\mu = \ln\frac{n}{s} + \frac{k_h}{k_s}\ln(s) - \frac{3}{4} + \pi\frac{2l^2k_h}{3q_w} \tag{13}$$

where $n = D_e/d_w$ (d_w = diameter of smear zone); $s = d_s/d_w$ (d_s = diameter of smear zone), k_h and k_s = horizontal permeabilities of the natural soil and smear zone, respectively. This method is more practical than the other methods since both vertical drains and their smear zones do not need to be represented in the equivalent plane strain analyses. The finite element mesh used for the equivalent plane strain analyses is illustrated in Fig. 7c. The equivalent vertical hydraulic conductivity k_{ve} is calculated as $1.98k_v$ by using Eq. (12). The finite element mesh consists of 474 15-noded triangular elements.

6. Results of numerical analyses

The 3D behaviour of the embankment on soft clay improved with PVDs was initially simulated using two different constitutive models (MCC and S-CLAY1S). Fig. 8 illustrates the surface settlements with time at the centre of the embankment. As shown in the figure, the S-CLAY1S model predicts marginally larger vertical settlements than the isotropic MCC model. Differences between two constitutive models are relatively minor immediately after construction of the embankment, but they become significant during consolidation. The MCC model predicts a final vertical settlement of about 0.77 m, whilst the prediction of about 1.21 m is given by the S-CLAY1S model after 25 years of consolidation. Accounting for anisotropy via a rotational hardening law and incorporating the effect of destructuration caused an important increase in the predicted final settlement. These results demonstrate that ignoring the effects of anisotropy and destructuration leads to underprediction of vertical displacements.

The predicted horizontal displacements versus depth under the crest of the embankment are shown in Fig. 9. Immediately after construction of the embankment both models give almost identical predictions of the horizontal displacements. Because the anisotropic model has the same elastic relationship as the isotropic MCC model, the S-CLAY1S model gives very similar predictions to the MCC model (maximum horizontal displacement u_x about 0.018 m). After consolidation the S-CLAY1S model predicts larger horizontal displacement (0.091 m) than the MCC models (0.078 m) at a depth of about 6.0 m.

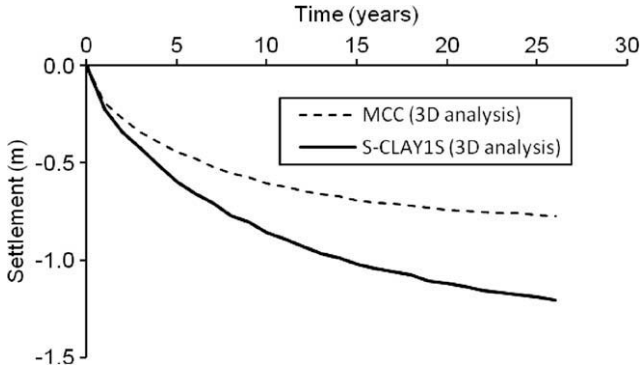

Fig. 8. Surface settlements with time at the center of the embankment.

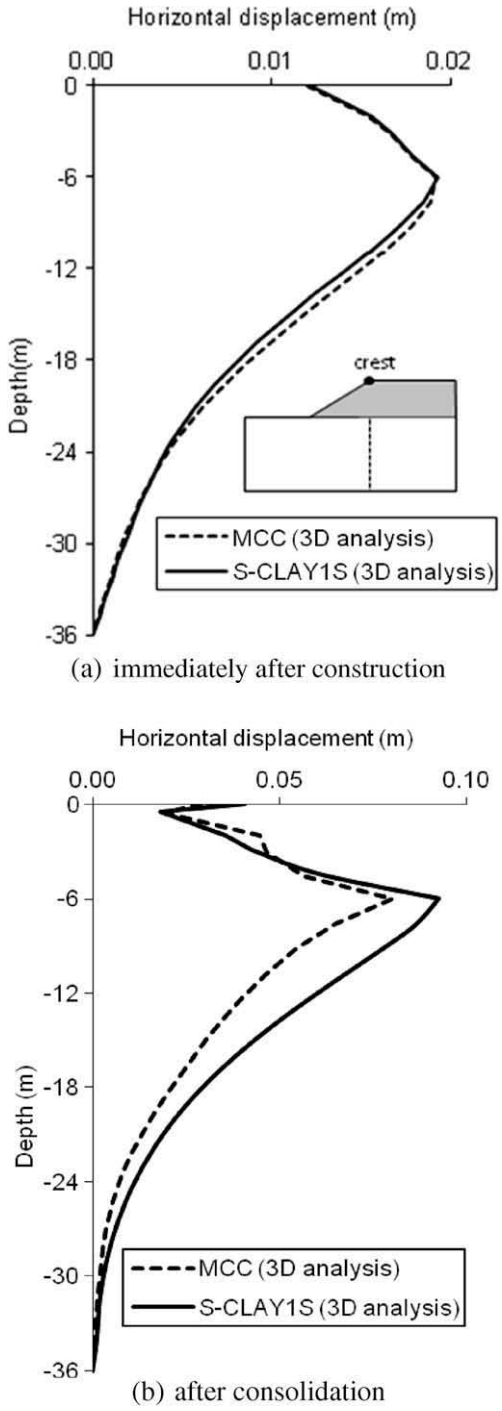

Fig. 9. Horizontal displacements underneath the crest of the embankment.

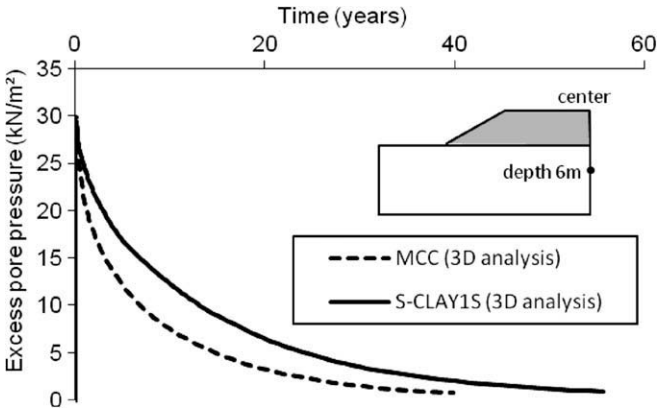

Fig. 10. Excess pore pressure variations with time below the center of the embankment (depth = 6 m).

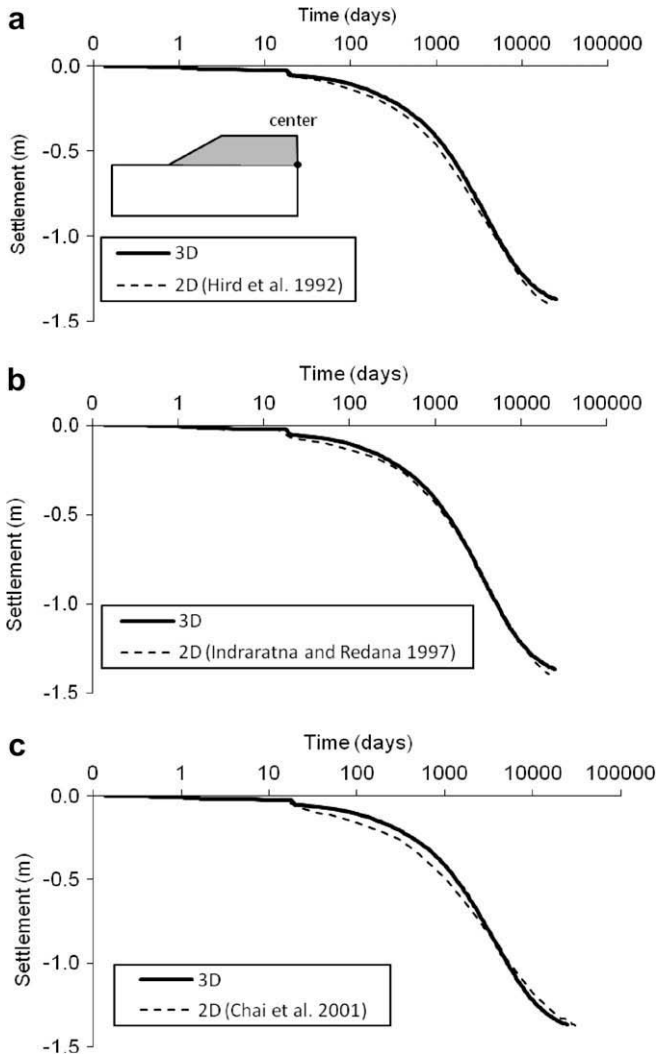

Fig. 11. Comparison of settlements predicted by 2D and 3D analyses for S-CLAY1S.

The predicted excess pore water pressure values at a depth of 6.0 m under the centreline of the embankment have been presented in Fig. 10. As expected, the pressure increases during the embankment construction and then gradually dissipates with time. Both models predict the same pressure (about 30 kPa at the end of construction) but the dissipation rate is faster with the isotropic MCC model than the anisotropic model.

2D plane strain analyses of the embankment are subsequently performed with three matching methods. The results have been plotted only for the S-CLAY1S model. The surface settlements predicted by 2D and 3D analyses at the centre of the embankment are compared in Fig. 11. During consolidation, the maximum differences between 3D and 2D predictions are about 4.2% with Hird et al. [14], 3% with Indraratna and Redana [15] and 6.5% with Chai et al. [16]. As shown in the figure, these matching methods reasonably predict the 3D results, but given the differences are different from one method to another. However, it should be emphasized that, in 3D analysis, the drain has been modelled by elastic solid

elements, but in 2D analyses, the stiffness of the drain is not considered and it treats just as the same as soft clay soil. This may cause discrepancy between the results.

The predicted horizontal displacements versus depth underneath the crest of the embankment are compared with the 3D results in Fig. 12 immediately after construction and consolidation. The predictions of Hird et al. [14] slightly underpredicted the horizontal displacements while the other two methods agree well with the 3D results (Fig. 12a). After consolidation, however, all matching methods predicted almost identical horizontal displacements and the results are in good agreement with the 3D results (Fig. 12b). The maximum horizontal displacement predicted by 3D analysis is about 0.091 m and it occurs at a depth of about 6.0 m. Three matching methods also predict the maximum value as about 0.10 m. The scatter in the plane strain predictions between 6 and 36 m depths is also in good agreement with the 3D results.

The excess pore water pressure values predicted by 2D plane strain analyses at a depth of 6 m below the ground surface under the centreline of the embankment are compared with the 3D predictions in Fig. 13. The predicted values are about 32.5 kN/m^2 with Hird et al. [14], 32.2 kN/m^2 with Indraratna and Redana [15] and 29 kN/m^2 with Chai et al. [16] whilst the 3D model predicts about 30 kN/m^2. The excess pore pressure dissipation rate after the construction differs from one method to another and 2D equivalent models predict a lower rate of dissipation during the consolidation.

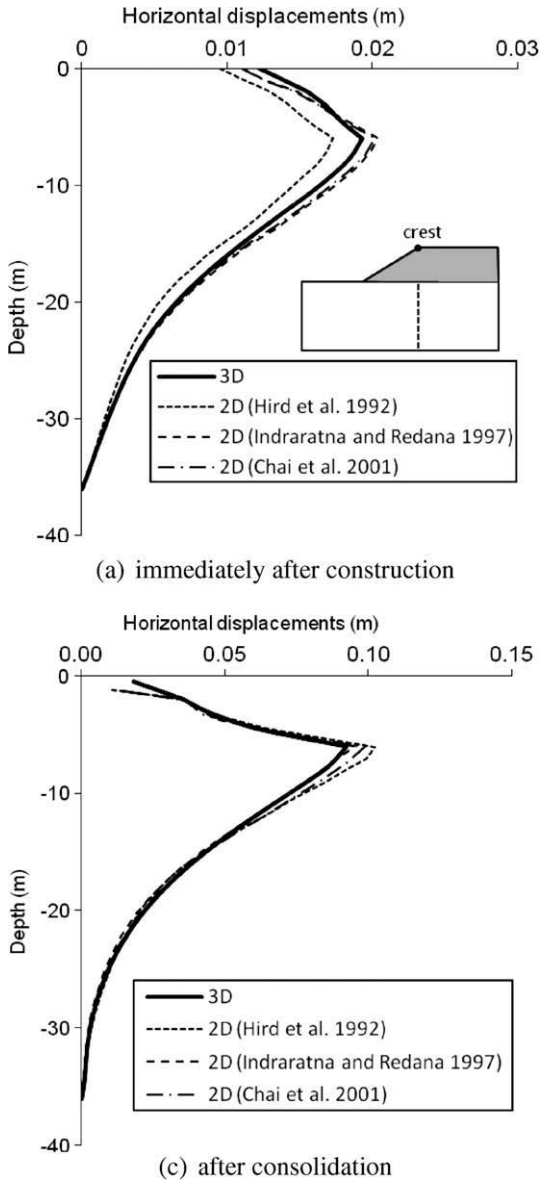

Fig. 12. Horizontal displacements underneath the crest of the embankment.

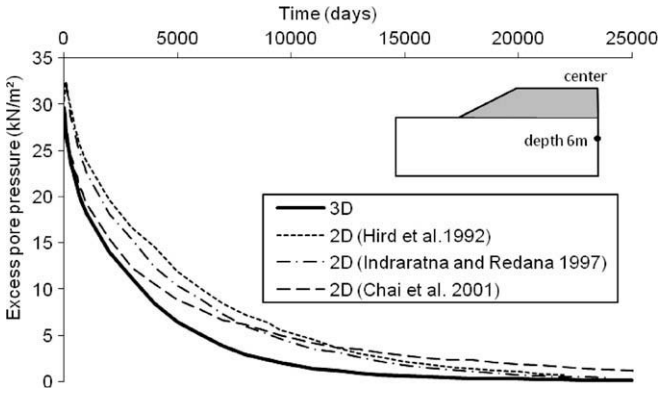

Fig. 13. Excess pore pressures below the centerline of the embankment (depth = 6 m).

7. Conclusion

This paper presents 3D finite element analyses of an embankment on PVD improved soft clay. A recently developed elasto-plastic S-CLAY1S model is used to represent the soft soil. The model accounts for initial and plastic strain induced anisotropy and, additionally, for interparticle bonding and degradation of bonds. For comparison, the embankment is also analysed with isotropic elasto-plastic MCC model. The numerical simulations demonstrate that the effects of anisotropy and micro-structure play an important role for this particular boundary value problem. These simulations also indicate that a 3D full scale analysis of an embankment on PVD-improved soft clays is very time consuming and not practical for engineers. The actual 3D behaviour of vertical drains is converted into equivalent plane strain conditions with three different matching techniques proposed by Hird et al. [14], Indraratna and Redana [15] and Chai et al. [16]. The results of 2D full-scale plane strain analyses are compared with the results of 3D numerical analysis. The equivalent plane strain analyses indicate that these matching techniques give acceptable results when real boundary conditions and complex elasto-plastic models are used in the finite element analyses. The differences vary from one method to another during consolidation. However, the match is found to be satisfactory for three methods. These techniques are useful tools for engineering practice and provide an easy way to analyse the behaviour of PVD-improved subsoil.

The matching method proposed by Indraratna and Redana [15] produced the best agreement with the 3D results with the maximum difference of about 3% in the predicted settlements. However, this procedure has an important disadvantage in that vertical drains and their smear zones need to be discretely represented in the finite element analyses. The matching method proposed by Chai et al. [16] is the simplest method since both vertical drains and their smear zones do not need to be modelled in the finite element analyses. The method represents the effect of vertical hydraulic conductivity of natural subsoil and the effect of radial drainage due to PVD using an equivalent vertical hydraulic conductivity k_{ve}. With the proposed method, the analysis of PVD-improved subsoil becomes the same as that for the unimproved case. However, the maximum difference in the predicted

settlements is about 6.5% as compared with the 3D results. This difference is larger than that predicted by the other two methods.

Acknowledgements

The work presented was carried out as part of a Marie Curie Research Training Network "Advanced Modelling of Ground Improvement on Soft Soils (AMGISS)" (MRTN-CT-2004-512120) supported by the European Community through the programme "Human Resources and Mobility". The paper was also supported by Cukurova University Scientific Research Project Directorate (Project no. MMF2008BAP9). The author wishes to thank Dr. Minna Karstunen, University of Strathclyde, Glasgow, UK, for her valuable comments and suggestions on this study.

References

[1] Duncan JM, Schaefer VR. Finite element consolidation analysis of embankments. Comput Geotech 1988;6(2):77–93.
[2] Bransby MF, Springman SM. 3-D finite element modelling of pile groups adjacent to surcharge loads. Comput Geotech 1996;19(4):301–24.
[3] Woodward PK, Berenji AP. Advanced numerical investigation of Terzaghi's superposition theory. Adv Eng Softw 2001;32(10–11):797–804.
[4] Salgado R, Lyamin AV, Sloan SW, Yu HS. Two- and three-dimensional bearing capacity of foundations in clay. Geotechnique 2004;54(5):297–306.
[5] Commend S, Geisera F, Crisinel J. Numerical simulation of earthworks and retaining system for a large excavation. Adv Eng Softw 2004;35:669–78.
[6] Bergado DT, Balasubramaniam AS, Fannin RJ, Holtz D. Prefabricated vertical drains (PVDs) in soft Bangkok clay: a case study of the new Bangkok International Airport project. Can Geotech J 2002;39:304–15.
[7] Kim YT, Lee SR. An equivalent model and back-analysis technique for modelling in situ consolidation behavior of drainage-installed soft deposits. Comput Geotech 1997;20(12):125–42.
[8] Indraratna B, Redana IW. Numerical modelling of vertical drains with smear and well resistance installed in soft clay. Can Geotech J 2000;37:132–45.
[9] Li AL, Rowe RK. Combined effects of reinforcement and prefabricated vertical drains on embankment performance. Can Geotech J 2001;38(1):1266–82.
[10] Chai JC, Miura N. Investigation of factors affecting vertical drain behavior. J Geotech Geoenviron Eng 1999;125(3):216–26.
[11] Borges JL. Three-dimensional analysis of embankments on soft soils incorporating vertical drains by finite element method. Comput Geotech 2004;31:665–76.
[12] Zeng GX, Xie KH. New development of vertical drain theories. In: Proceedings of the 12th ICSMFE, vol. 2, Rio De Janeiro; 1989. p. 1435–8.
[13] Cheung YK, Lee PKK, Xie KH. Some remarks on two- and three-dimensional consolidation analysis of sand-drained ground. Comput Geotech 1991;12(1):73–87.
[14] Hird CC, Pyrah IC, Russell D. Finite element modelling of vertical drains beneath embankments on soft ground. Geotechnique 1992;42(3):499–511.
[15] Indraratna B, Redana IW. Plane strain modeling of smear effects associated with vertical drains. J Geotech Geoenviron Eng 1997;123(5):474–8.
[16] Chai JC, Shen SL, Miura N, Bergado DT. A simple method of modeling PVD improved subsoil. J Geotech Geoenviron Eng 2001;127(11):965–72.
[17] Karstunen M, Krenn H, Wheeler SJ, Koskınen M, Zentar R. The effect of anisotropy and destructuration on the behaviour of murro test embankment. Int J Geomech 2005;5(2):87–97.
[18] Roscoe KH, Burland JB. On the generalized stress–strain behaviour of 'wet' clay. Engineering plasticity. Cambridge University Press; 1968. p. 553–609.
[19] Wheeler SJ, Näätänen A, Karstunen M, Lojander M. An anisotropic elasto plastic model for soft clays. Can Geotech J 2003;40:403–18.
[20] Koskinen M, Karstunen M, Wheeler SJ. Modelling destructuration and anisotropy of a natural soft clay. In: Proc. of the fifth European conf. num. meth. in geotech. engng., Paris, Presses De L'enpc/Lcpc; 2002. p. 11–20.
[21] Koskinen M, Zentar R, Karstunen M. Anisotropy of reconstituted poko clay. In: Proc. of the eighth int. symp. on num. models in geomech. (NUMOG), Rome; 2002. p. 99–105.
[22] Zentar R, Karstunen M, Wheeler SJ. Influence of anisotropy and destructuration on undrained shearing of natural clays. In: Proc. of the fifth European conf. on num. meth. in geotech. engng. (NUMGE), Paris; 2002. p. 21–26.
[23] Karstunen M, Koskinen M. Plastic anisotropy of soft reconstituted clays. Can Geotech J 2008;45:314–28.
[24] Karstunen M, Wiltafsky C, Krenn H, Scharinger F. Modelling the behaviour of an embankment on soft clay with different constitutive models. Int J Numer Anal Method Geomech 2006;30:953–82.
[25] Taylor DW. Fundamentals of soil mechanics. New York: Wiley; 1948.
[26] Tavenas F, Jean P, Leblond P, Leroueil S. The permeability of natural clays. Part II: Permeability characteristics. Can Geotech J 1983;20(4):645–60.
[27] Hawlader BC, Imai G, Muhunthan B. Numerical study of the factors affecting the consolidation of clay with vertical drains. Geotext Geomem 2002;20:213–39.
[28] Jamiolkowski M, Lancellotta R. Consolidation by vertical drains: uncertainties involved in prediction of settlement rates. Proc. of the 10th int. conf. soil mech. and found. eng., vol. 4. Rotterdam, The Netherlands: Balkema; 1981. p. 593–5.
[29] Madhav R, Park YM, Miura N. Modelling and study of smear zones around band shaped drains. Soil Found 1993;33(4):135–47.
[30] Bergado DT, Mukherjee K, Alfaro MC, Balasubramaniam AS. Prediction of vertical-band-drain performance by the finite-element method. Geotext Geomem 1993;12:567–86.
[31] Indraratna B, Balasubramaniam AS, Ratnayake P. Performance of embankment stabilized with vertical drains on soft clay. J Geotech Eng ASCE 1994;120(2):257–73.
[32] Rixner JJ, Kraemer SR, Smith AD. Prefabricated vertical drains. Engrg Guidelines, Federal Highway Admin, Report no. Fhwa-Rd-86/169, Washington, DC. 433pp.
[33] Hansbo S. Consolidation of fine-grained soils by prefabricated drains. In: Proc. of the 10th int. conf. on soil mech. and found. engng., vol. 3, Stockholm; 1981. p. 677–82.
[34] Yildiz A, Karstunen M, Krenn H. Numerical modelling of vertical drains with advanced constitutive models. In: Proc. of the sixth European conf. on num. meth. in geotech. engng., Graz, Austria, September 6–8; 2006.
[35] Carrillo N. Simple two-and three-dimensional cases in the theory of consolidation of soils. J Math Phys 1942;21:1–5.